J. Fluid Mech. (2001), *vol.* 449, *pp.* 291–300.
DOI: 10.1017/S0022112001006243 Printed in the United Kingdom

Periodic motion embedded in plane Couette turbulence: regeneration cycle and burst

By GENTA KAWAHARA[1] AND SHIGEO KIDA[2]

[1]Department of Mechanical Engineering, Ehime University, Matsuyama 790–8577, Japan

[2]Theory and Computer Simulation Center, National Institute for Fusion Science, Toki 509–5292, Japan

(Received 14 August 2001)

Two time-periodic solutions with genuine three-dimensional structure are numerically discovered for the incompressible Navier–Stokes equation of a constrained plane Couette flow. One solution with strong variation in spatial and temporal structure exhibits a full regeneration cycle, which consists of the formation and breakdown of streamwise vortices and low-velocity streaks; the other one, of gentle variation, represents a spanwise standing-wave motion of low-velocity streaks. These two solutions are unstable and the corresponding periodic orbits in the phase space are connected with each other. A turbulent state wanders around the strong one for most of the time except for occasional escapes from it. As a result, the mean velocity profile and the root-mean-squares of velocity fluctuations of the plane Couette turbulence agree very well with the temporal averages of those of this periodic motion. After an occasional escape from the strong solution, the turbulent state reaches the gentle periodic solution and returns. On the way back, it experiences an overshoot accompanied by strong turbulence activity like an intermittent bursting phenomenon.

1. Introduction

Since the famous experiments by Reynolds (1883) much effort has been devoted to understanding and controlling fluid turbulence. However, the lack of a simple spatiotemporal description of such a huge irregular system with strong nonlinearity has impeded the elucidation of the structural and dynamical properties of turbulent flows. Indeed complex and chaotic behaviour in both space and time is the primary characteristic of fully developed turbulence, yet there is numerous experimental and numerical evidence for the existence of striking coherent motions and structures (see Cantwell 1981; Robinson 1991). Coherent structures are known, at least qualitatively, to play key roles in the transport of passive materials, momentum and energy (Kim, Kline & Reynolds 1971), the sustenance of turbulence activity (Panton 1997), the building of intermittent fluctuations, and so forth. The presence of the coherent structures can help the understanding of turbulent flows because they show simpler behaviour than turbulence itself.

The number of active modes in any turbulent motion of a viscous fluid in a finite domain is always finite, since the small-scale motion is smoothed out by viscosity (see Constantin *et al.* 1985). Therefore, a turbulent flow may be regarded as a dynamical system of finite dimension. In terms of dynamical-system theory, the spatiotemporal coherent structure in turbulence may be thought of as a low-dimensional manifold, in the neighbourhood of which the dynamical system spends

a substantial fraction of time (see Jiménez 1987). In chaotic systems of low degrees of freedom the infinite number of unstable periodic orbits, which are embedded in a chaotic attractor (Eckmann & Ruelle 1985), have been shown to provide a useful characterization of structure and dynamics of the attractor (Auerbach *et al.* 1987; Christiansen, Cvitanović & Putkaradze 1997). In this context, the simplest description, in phase space, of spatiotemporal coherence in turbulence should be given by a periodic saddle orbit embedded in a turbulent attractor, though it is much more difficult to find an unstable periodic orbit in that high-dimensional system.

In their numerical simulations of plane Poiseuille turbulence Jiménez & Moin (1991) minimized the streamwise and spanwise dimensions of a computational periodic box while sustaining turbulence activity. By using the same technique, Hamilton, Kim & Waleffe (1995) lowered the Reynolds number further to reduce the degrees of freedom of plane Couette turbulence. In this highly constrained system they reported a recurrent dynamical process of formation and breakdown of near-wall coherent structures, such as streamwise vortices and low-velocity streaks, in a qualitative way. It is known that the regeneration cycle is generally present in near-wall turbulence to sustain coherent structures (Panton 1997; Jiménez & Pinelli 1999). Waleffe (1997) described the three phases of the regeneration cycle (i.e. formation of streaks, streak instability and regeneration of vortices) in terms of a linear or nonlinear theory, and proposed a low-dimensional model to interpret the interactions between the three phases. However, a theoretical description of the whole regeneration cycle based on the full equations has not been established yet.

In this paper we present two new unstable periodic solutions of the incompressible Navier–Stokes equation which characterize a constrained plane Couette turbulence. The method of direct numerical simulation and the parameter setting are described in § 2. One of the periodic solutions of strong variation is obtained by an iterative method in § 3. It is shown that this solution is embedded in the chaotic trajectories of the Couette turbulence and exhibits the main characteristics of turbulence which include the full regeneration cycle and the mean velocity profile. Another periodic solution of gentle variation is found in § 4, where its heteroclinic connections with the strong periodic solution and relevance to the bursting phenomenon are discussed. Finally, our concluding remarks are given in § 5.

2. Numerical Couette turbulence

An unstable periodic orbit, if one exists, may be relatively easily obtained in the above-mentioned constrained turbulence of lower degrees of freedom. We have therefore performed direct numerical simulations of the incompressible Navier–Stokes equation, by using a spectral method, for the same constrained Couette turbulence as investigated by Hamilton *et al.* (1995). The numerical scheme for the simulation is essentially that used by Kim, Moin & Moser (1987), and the volume flux is set to be zero. The dealiased Fourier expansions are employed in the streamwise (x) and spanwise (z) directions, and the Chebyshev-polynomial expansion in the wall-normal (y) direction. Numerical computations are carried out on 8448 ($= 16 \times 33 \times 16$ in x, y, and z) grid points at Reynolds number $Re \equiv Uh/\nu = 400$, where U is half the difference of the two wall velocities, h is half the wall separation, and ν is the kinematic viscosity of fluid. The numerical accuracy of this grid resolution has been checked by doubling the resolution. The Reynolds number based on the mean friction velocity u_τ and h is $Re_\tau = 37.1$. The streamwise and spanwise computational periods are $L_x = 5.513h$ ($= 188\nu/u_\tau$) and $L_z = 3.770h$ ($= 128\nu/u_\tau$),

respectively. The energy is injected through the frictional force on the moving walls and consumed at small scales over the whole flow field by viscous dissipation. The energy input $I \equiv \int_0^{L_x}\int_0^{L_z}(\partial u/\partial y|_{y=-h} + \partial u/\partial y|_{y=+h})\,\mathrm{d}x\,\mathrm{d}z/(2L_xL_zU/h)$ and dissipation $D \equiv \int_0^{L_x}\int_{-h}^{+h}\int_0^{L_z}|\boldsymbol{\omega}|^2\mathrm{d}x\,\mathrm{d}y\,\mathrm{d}z/(L_xL_zU^2/h)$ per unit time vary in a complicated way in time, where u is the streamwise velocity and $\boldsymbol{\omega}$ is the vorticity vector. Their temporal averages, which are substantially larger than the corresponding ones in a laminar state (see figure 1), are the same because the turbulence is statistically stationary.

In the present numerical scheme the dependent variables are 31 Chebyshev coefficients for the mean streamwise and spanwise components of velocity, 7424 ($= 16 \times 29 \times 16$) Fourier–Chebyshev–Fourier coefficients for the wall-normal velocity, and 7936 ($= 16 \times 31 \times 16$) Fourier–Chebyshev–Fourier coefficients for the wall-normal vorticity. The number N of degrees of freedom of the present dynamical system is therefore 15 422. An instantaneous state of the flow field and its temporal evolution should be represented respectively, in principle, as a point and its trajectory in the N-dimensional phase space spanned by all the independent variables. In figure 1, we plot, with a grey line, a projection of the turbulence trajectory over a period of $10^4h/U$ on the two-dimensional subspace spanned by the total energy input rate I and dissipation rate D normalized by those for a laminar state. Green dots are attached at intervals of $2h/U$. The orbit generally tends to turn clockwise. The energy input and dissipation rates are in balance on the dashed diagonal. Whenever a flow state is above (or below) the diagonal, the total kinetic energy is decreasing (or increasing). The variation of the trajectory, which is confined in a finite domain, is far from periodic. On the contrary, the frequency spectrum of the total kinetic energy is continuous (figure is omitted), which suggests that the orbit may be in a chaotic state.

3. Periodic motion embedded in turbulence

Motivated by previous work on finding periodic orbits embedded in a strange attractor in many simple dynamical systems and on the observations of recurrent dynamical processes in the present system, we searched for a periodic orbit which might be embedded in the turbulent flow. We employ a standard direction-set method for iteration to minimize the Euclidean distance between successive cross-points of the orbit on a plane $\mathrm{Im}(\widetilde{\omega}_{y\,0,0,1}) = -0.1875U/h$ in the N-dimensional phase space, where $\mathrm{Im}(\widetilde{\omega}_{y\,0,0,1})$ is the imaginary part of the Fourier–Chebyshev–Fourier coefficient of the wall-normal vorticity for the zero streamwise wavenumber, the zeroth order Chebyshev polynomial, and the $2\pi/L_z$ spanwise wavenumber. A flow state at an arbitrary time when the turbulence trajectory is travelling more or less periodically in the phase space was chosen as the first guess for the iteration.

The iteration was continued until the distance between successive cross-points fell within 1% of that from the origin of the earlier one. (However, a much lower threshold may be necessary for stability analysis of a periodic orbit.) A periodic orbit thus obtained is drawn in figure 1 with a closed red line, the period of which is $64.7h/U$ ($= 188\nu/u_\tau^2$). Green dots on the turbulence trajectory are much denser near the periodic orbit, implying that the turbulent state approaches it very frequently. An example of such a close approach is shown with a yellow line which is a cut of the turbulence trajectory. The turbulent state approaches the periodic orbit and follows it closely during one or two periods. The approaches to the periodic orbit have been confirmed not only in this (I, D)-plane but also in other subspaces, during which the spatiotemporal structures of the turbulent flow resemble remarkably those

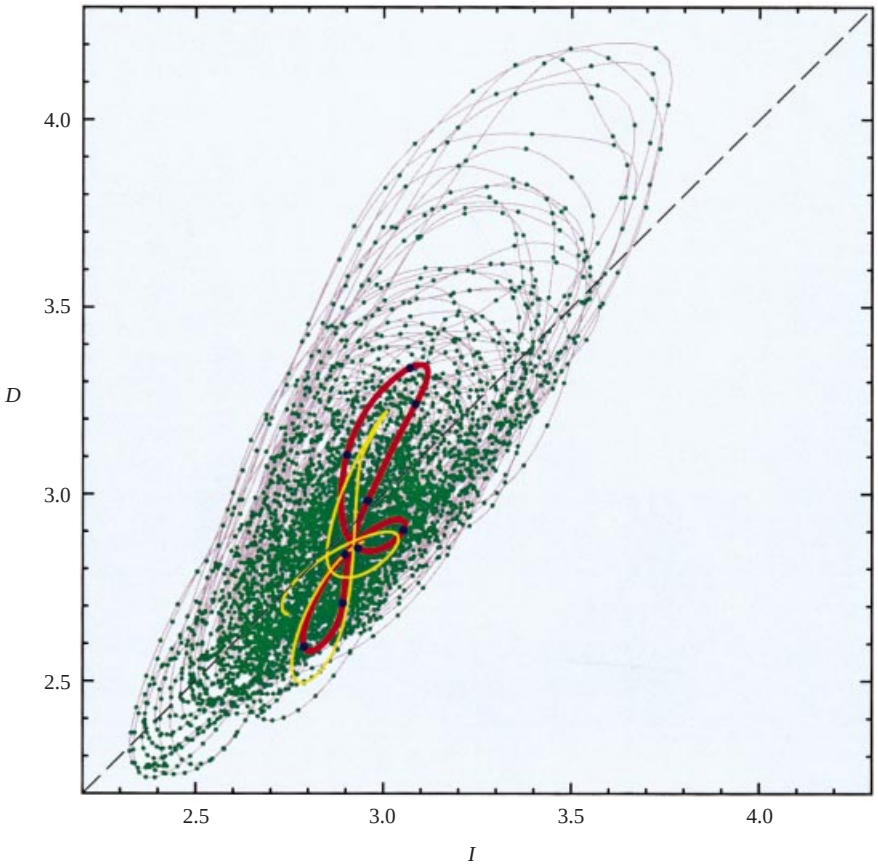

FIGURE 1. Two-dimensional projections of a turbulent and a periodic orbit. The horizontal and vertical axes respectively represent total energy input rate I and dissipation rate D normalized by those for a laminar state. The grey line shows the turbulence trajectory, to which green dots are attached at intervals of $2h/U$. A closed red line denotes a periodic orbit. A cut of the turbulence trajectory is coloured yellow to show a typical approach to the periodic orbit. All the orbits generally turn clockwise. Nine blue dots on the periodic orbit indicate the phases of panels (a)–(i) in figure 2. The energy input and dissipation rates are in balance on the dashed diagonal.

for the periodic flow (see figure 2). However, the approach does not continue forever. The turbulence trajectory will go away, sooner or later, from the periodic orbit. In other words, this periodic orbit is a saddle. Occasionally, the turbulent state comes to high-dissipation ($D > 4$, say) regions. This migration will be discussed in § 4 in relation to the burst which activates small-scale motions to enhance the energy dissipation (Kim *et al.* 1971). The present extraction of a periodic orbit may offer the first (to our knowledge) direct demonstration of the existence of a periodic motion embedded in a turbulent flow, at least for this constrained case.

A full cycle of the temporal evolution of spatial structure of the periodic solution is depicted in figure 2(a–i) at nine sequential phases indicated by blue dots on the periodic orbit in figure 1. The phase of figure 2(a) corresponds to the blue dot at the time of the least input and dissipation rates. Typical near-wall coherent structures are clockwise (or counter-clockwise) streamwise (x) vortices visualized by the red (or blue) iso-surfaces of the Laplacian of pressure (see also the cross-flow velocity vectors), and are streamwise streaks of relatively low streamwise velocity represented

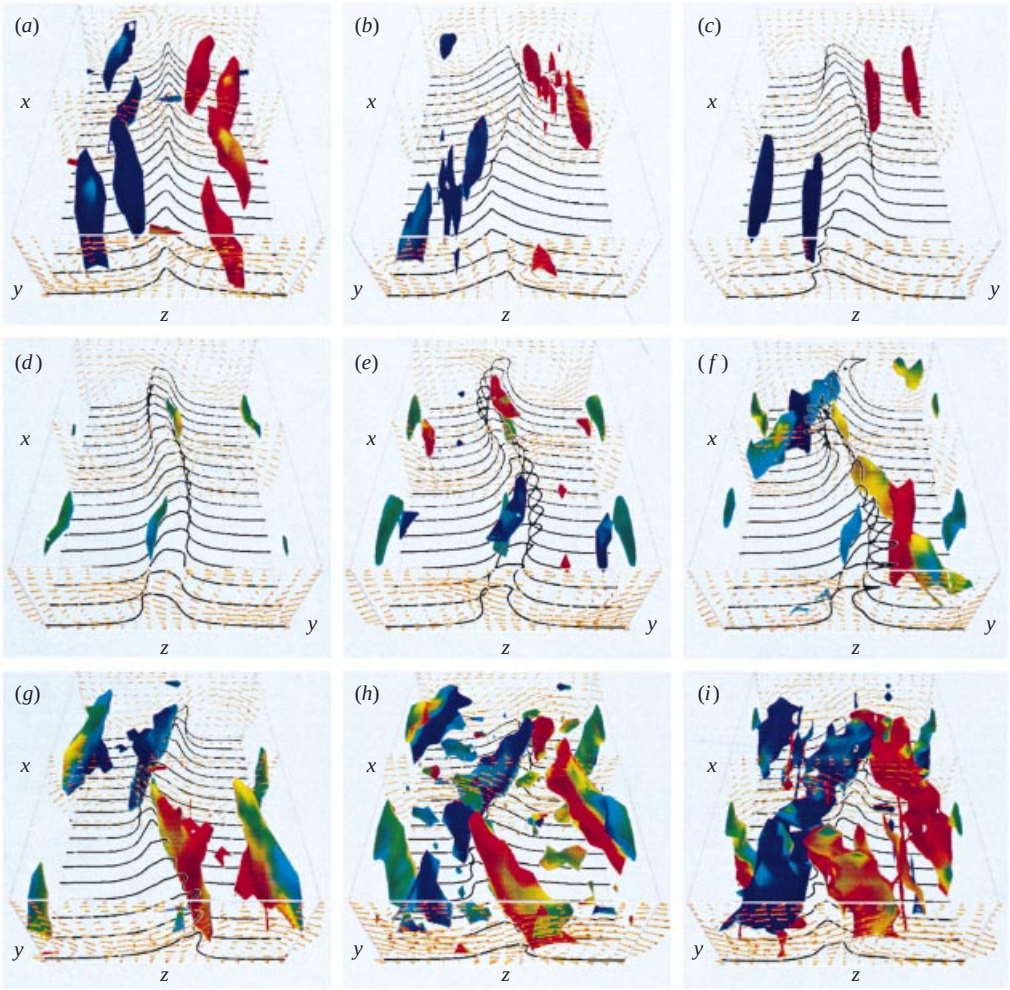

FIGURE 2. A full cycle of a time-periodic flow. Flow structures are visualized in the whole spatially periodic box ($L_x \times 2h \times L_z$) over one full cycle at nine times shown with blue dots in figure 1, where panels (*a*) and (*f*) correspond respectively to the lowest and highest dots there. Time increases from (*a*) to (*i*) by $7.2h/U$. The upper (or lower) wall moves into (or out of) the page at velocity U (or $-U$). Vortex structures are represented by iso-surfaces of the Laplacian of pressure, $\nabla^2 p = 0.15\rho U^2/h^2$, where ρ is the mass density of the fluid (see Tanaka & Kida 1993). Colour on the iso-surfaces of $\nabla^2 p$ indicates the sign of the streamwise (x) vorticity: red is positive (clockwise), blue is negative (counter-clockwise), and green is zero. Cross-flow velocity vectors and contours of the streamwise velocity at $u = -0.3U$ are also shown on cross-flow planes $x = \text{const}$.

by lifted iso-contours in (y, z)-planes (Jeong *et al.* 1997). The dynamics of the periodic flow is described by a cyclic sequence of events which consists of (i) the formation and development of low-velocity streaks through the advection of streamwise velocity in the cross-flow induced by decaying streamwise vortices (figure 2*a–d*), (ii) the bending along the streamwise direction and tilting in the spanwise (z) direction of the streaks followed by the regeneration of streamwise vortices (figure 2*e–g*), and (iii) the breakdown of streaks and the violent development of streamwise vortices (figure 2*h,i*). This cyclic sequence is completely consistent with a previously reported regeneration cycle (Hamilton *et al.* 1995; Waleffe 1997).

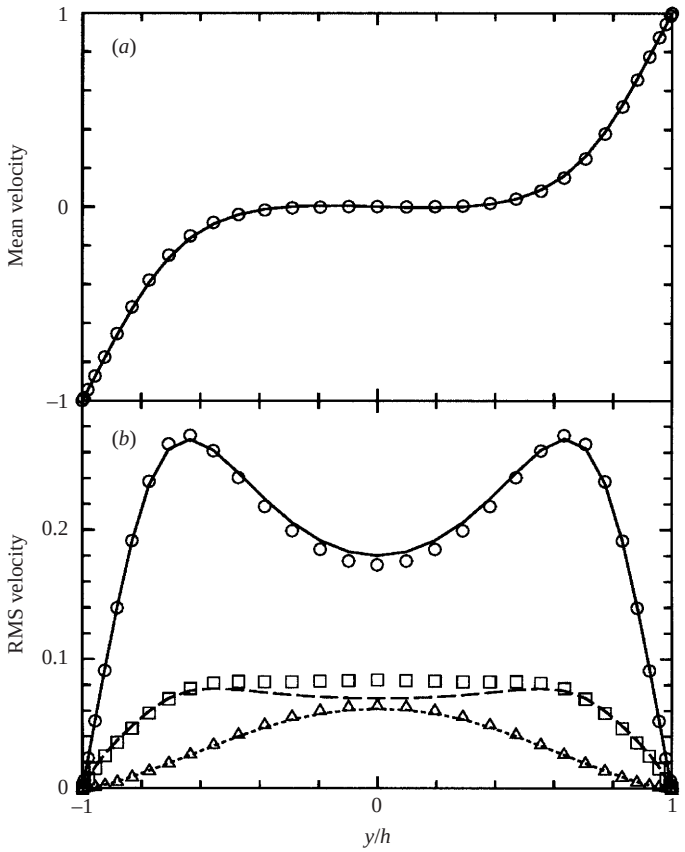

FIGURE 3. Comparison of the mean and RMS velocities between a time-periodic and a turbulent flow. (*a*) The mean streamwise velocity normalized by U versus the wall-normal coordinate y/h. (*b*) The RMS velocities normalized by U versus y/h. Symbols and lines stand for the time-periodic and turbulent flows, respectively. Circles and a solid line indicate the streamwise component, triangles and a dotted line the wall-normal component, and squares and a dashed line the spanwise component. Averages are taken over planes parallel to the walls, $y = \text{const.}$, and over one time period $64.7h/U$ for the time-periodic flow or over a period of $6 \times 10^4 h/U$ for the turbulent flow.

Figures 3(*a*) and 3(*b*) compare the mean and RMS (root-mean-square) velocities for the time-periodic flow (symbols) with those for the turbulent flow (lines), where both the mean and RMS velocities are scaled by U. The mean streamwise velocity for the time-periodic flow is in very good agreement with that for the turbulent flow. It is surprising and remarkable that even the RMS velocities of streamwise, wall-normal, and spanwise components for the time-periodic flow coincide with those for the turbulent flow. Excellent agreement in all the RMS vorticities and the Reynolds shear stress, has also been confirmed. This is expected because the turbulent state spends most of the time in the neighbourhood of the periodic orbit.

4. Periodic motion of gentle variations

As seen in figure 1, a turbulence state passes highly active regions at rare intervals. This is reminiscent of the burst, which is an intermittent high-activity phenomenon. A detailed inspection of the turbulence trajectory reveals that such highly active regions are almost always reached from rather low energy input and dissipation states. From

this point of view, it is instructive to recall a similar behaviour observed in plane Poiseuille turbulence. Recently, Itano & Toh (2001) have discovered, by a shooting method, an unstable travelling-wave solution of three-dimensional structure to the Navier–Stokes equation for a plane Poiseuille flow. This solution is laminar and less dissipative than a turbulent state. It corresponds to a saddle point in the phase space. A turbulence trajectory occasionally closely approaches the saddle point and leaves rapidly in some unpredictable direction. They argue that this sequence of events may describe a bursting process. Transient movements of a turbulence state toward relatively quiescent regions of low energy input and dissipation are observed in the present system as well (see figure 1). This motivated us to seek an unstable fixed point related to the bursting process for a plane Couette flow. By employing a shooting method similar to theirs, we encountered a Nagata's (1990) (lower-branch) steady solution (see the black dot in figure 4) for a longer streamwise period L_x. This steady solution bifurcates into a periodic orbit at $L_x < 6.1h$. It makes an orbit of period $85.5h/U$ $(= 248v/u_\tau^2)$ in our case ($L_x = 5.513h$).

This periodic orbit is plotted as a closed blue circle in figure 4. The red curve is taken from figure 1. The blue orbit is located at substantially lower levels of the energy input and dissipation rates than the red, and its amplitude of oscillation is quite small. The mean velocity profile for this gentle periodic solution is closer to that for a laminar state, and the wall-normal and spanwise RMS velocities, the maximum values of which are respectively only $0.016U$ and $0.028U$, are much less than those for the turbulent and strong solutions everywhere. The streamwise RMS velocity has a relatively large maximum value $0.322U$ at $y = \pm 0.383h$, but in the near-wall region ($|y| > 0.6h$) it is also less than that for the turbulent and strong solutions. An example of a bursting trajectory (not included in figure 1) is shown by a grey line with green dots attached at intervals of $2h/U$. A turbulent state, which was wandering around the red periodic orbit for a while, begins to escape from it and moves slowly toward the blue one. At some distance from it, the turbulent state stops and makes a U-turn back to the red orbit. Soon after, the turbulent state is accelerated and thrown far away to very-high energy input and dissipation regions before coming back to the neighbourhood of the original red periodic orbit. This is a typical bursting trajectory.

Since the bursting process is 'a round trip' between the two periodic solutions in the phase space, it is interesting to see how they are connected. To find the connection we trace numerically those orbits that start somewhere close to each of the periodic solutions. In practice, 3–5% random perturbations are added to the red periodic orbit, while only the coefficients for the x-dependent Fourier modes are multiplied by a constant c ($1 < c \leqslant 1.1$) to set up a starting point near the blue periodic orbit. The orbits are very variant, especially around the red periodic solution, depending upon the starting points. In figure 5, we plot two typical connecting orbits, where the green and purple lines start near the blue and red periodic solutions, respectively. The time is marked with dots at intervals of $2h/U$. These connections have also been confirmed in other projection planes, suggesting the existence of heteroclinic connections between the two periodic solutions. Note that these orbits exibit more violent and complicated structures around the red periodic solution. It is conjectured that the bursting trajectories run more or less along these heteroclinic connections.

5. Concluding remarks

Two unstable time-periodic solutions of different natures have been obtained numerically for a constrained plane Couette flow. One with strong variation, i.e. the red

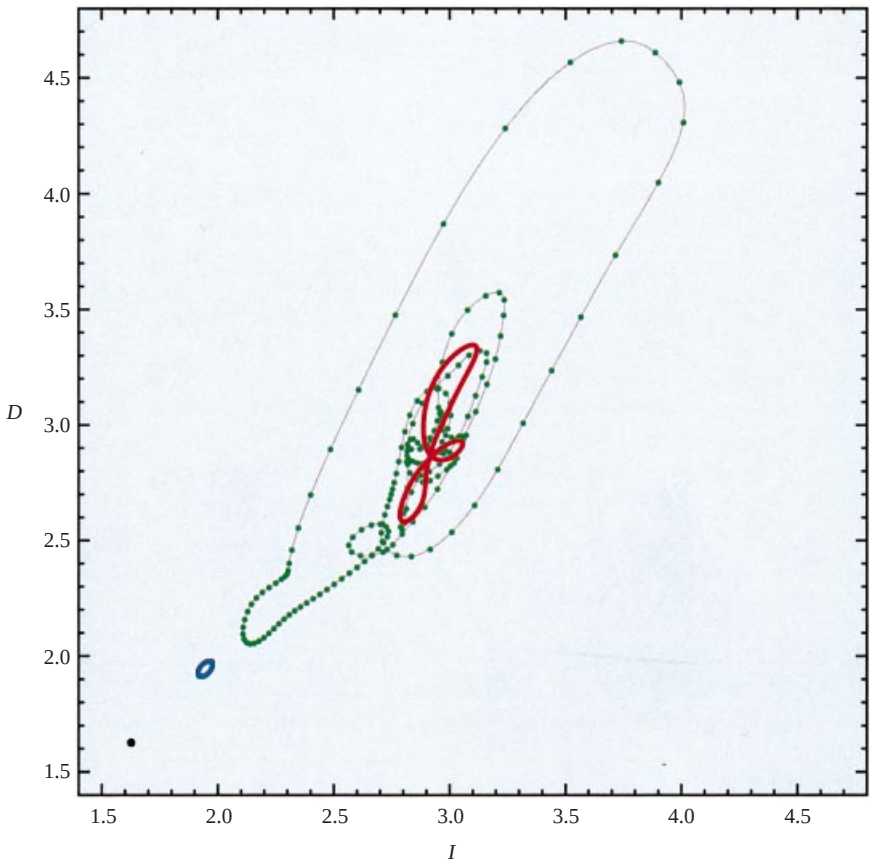

FIGURE 4. Two-dimensional projections of a bursting trajectory and two periodic orbits in the (I, D)-plane. A bursting trajectory is drawn over a period of $400h/U$ with a grey line to which green dots are attached at intervals of $2h/U$. Closed blue and red lines denote two periodic orbits. The black dot represents a Nagata's (1990) (lower-branch) steady solution for the longer streamwise period ($L_x = 6.189h$) which bifurcates into the blue orbit. The red orbit is taken from figure 1.

periodic orbit in figures 1, 4 and 5, has rich spatiotemporal properties and shares the full regeneration cycle of the near-wall coherent structures in plane Couette turbulence. The turbulent state spends most of the time around this periodic solution, and occasionally escapes from it to lead a burst. Usually the word 'coherent structure' expresses the spatial coherence, but it may be more appropriate to add it to the meaning of the temporal coherence as well. The above periodic solution gives a concrete example of both spatial and temporal coherent structures in a turbulent flow.

The other periodic solution of gentle variation, i.e. the blue periodic orbit in figures 4 and 5, is less dissipative than a turbulent state. A Nagata's (1990) (lower-branch) steady solution found for longer streamwise periods L_x, which takes the form of wavy low-velocity streaks flanked by staggered streamwise vortices of alternating signs, bifurcates into this gentle periodic solution at $L_x < 6.1h$. The small oscillation of this solution expresses a spanwise standing-wave motion of the low-velocity streaks, in which it goes to and fro between two (equivalent) Nagata's steady solutions that differ from each other only by a half period ($L_x/2$) shift in the streamwise direction. A related but different periodic solution was found by Clever & Busse (1997). Nagata's

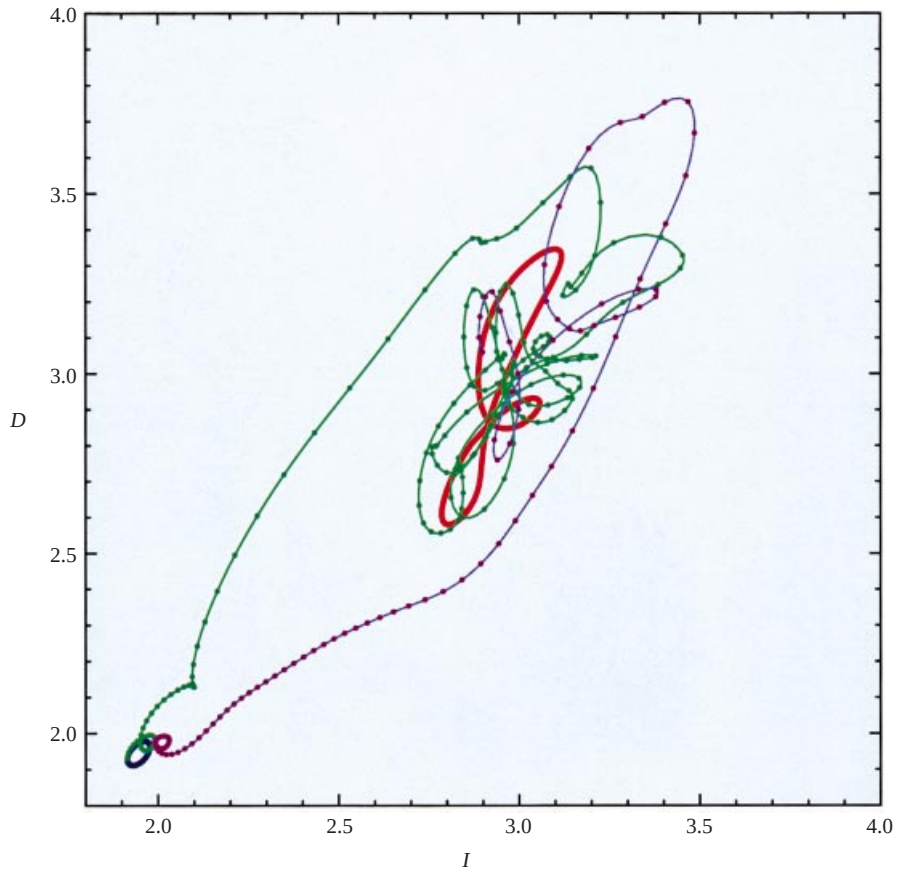

FIGURE 5. Heteroclinic connections between two periodic solutions in the (I, D)-plane. Closed blue and red lines denote two periodic solutions. A green (or purple) line represents a connecting orbit which starts near the blue (or red) periodic solution and approaches the red (or blue) one. The time is marked with dots at intervals of $2h/U$.

(upper-branch) steady solutions bifurcate into this periodic solution at $Re \approx 150$. The spatial structure of this solution is not much different from that of the steady solution throughout the cycle except for a slight variation of the amplitude. There are heteroclinic connections between our two periodic solutions, which may serve as the paths of the bursting trajectories.

Schmiegel (1999) found a number of new steady solutions for plane Couette flow in a larger periodic box ($L_x = 12.566h$, $L_z = 6.283h$) and suggested that a turbulent state is formed by a complex framework of heteroclinic connections between them. Examination of the relevance of the present strong periodic solution with known steady solutions, such as Nagata's (upper-branch) solution and Schmiegel's solutions, is left for a future study.

Finally, we make some remarks on the spatial symmetries (see Nagata 1990; Clever & Busse 1997) of the present solutions, that is (i) the reflection with respect to the plane $z = 0$ and a streamwise shift by $L_x/2$, and (ii) the 180° rotation around the line $x = y = 0$ and a spanwise shift by $L_z/2$. These symmetries seem to be realized mainly because the flow is constrained, namely at a low Reynolds number in the smallest periodic box. One or both symmetries may be broken at a higher Reynolds number

or in a larger periodic box. Many other new periodic motions might also appear, some localized near only a single wall. Nevertheless, the present periodic solutions may provide us with simple spatiotemporal characterization of turbulence, which are a crucial base for understanding turbulent flows, at least in constrained plane Couette flows.

We are grateful to Professor S. Toh for providing his simulation code used in this study. This work has been partially supported by the Grant-in-Aid for Scientific Research on Priority Areas (B) from the Ministry of Education, Culture, Sports, Science and Technology of Japan.

REFERENCES

Auerbach, D., Cvitanović, P., Eckmann, J.-P., Gunaratne, G. & Procaccia, I. 1987 Exploring chaotic motion through periodic orbits. *Phys. Rev. Lett.* **58**, 2387–2389.

Cantwell, B. J. 1981 Organized motion in turbulent flow. *Ann. Rev. Fluid Mech.* **13**, 457–515.

Christiansen, F., Cvitanović, P. & Putkaradze, V. 1997 Spatiotemporal chaos in terms of unstable recurrent patterns. *Nonlinearity* **10**, 55–70.

Clever, R. M. & Busse, F. H. 1997 Tertiary and quaternary solutions for plane Couette flow. *J. Fluid Mech.* **344**, 137–153.

Constantin, P., Foias, C., Manley, O. P. & Temam, R. 1985 Determining modes and fractal dimension of turbulent flows. *J. Fluid Mech.* **150**, 427–440.

Eckmann, J.-P. & Ruelle, D. 1985 Ergodic theory of chaos and strange attractors. *Rev. Mod. Phys.* **57**, 617–656.

Hamilton, J. M., Kim, J. & Waleffe, F. 1995 Regeneration mechanisms of near-wall turbulence structures. *J. Fluid Mech.* **287**, 317–348.

Itano, T. & Toh, S. 2001 The dynamics of bursting process in wall turbulence. *J. Phys. Soc. Japan* **70**, 701–714.

Jeong, J., Hussain, F., Schoppa, W. & Kim, J. 1997 Coherent structures near the wall in a turbulent channel flow. *J. Fluid Mech.* **332**, 185–214.

Jiménez, J. 1987 Coherent structures and dynamical systems. In *Proc. 1987 Summer Program of Center for Turbulence Research, Stanford University*. CTR-S87, pp. 323–324.

Jiménez, J. & Moin, P. 1991 The minimal flow unit in near-wall turbulence. *J. Fluid Mech.* **225**, 213–240.

Jiménez, J. & Pinelli, A. 1999 The autonomous cycle of near-wall turbulence. *J. Fluid Mech.* **389**, 335–359.

Kim, H. T., Kline, S. J. & Reynolds, W. C. 1971 The production of turbulence near a smooth wall in a turbulent boundary layer. *J. Fluid Mech.* **50**, 133–160.

Kim, J., Moin, P. & Moser, R. 1987 Turbulence statistics in fully developed channel flow at low Reynolds number. *J. Fluid Mech.* **177**, 133–166.

Nagata, M. 1990 Three-dimensional finite-amplitude solutions in plane Couette flow: bifurcation from infinity. *J. Fluid Mech.* **217**, 519–527.

Panton, R. (Ed.) 1997 *Self-Sustaining Mechanisms of Wall Turbulence*. Computational Mechanics Publications.

Reynolds, O. 1883 An experimental investigation of the circumstances which determine whether the motion of water shall be direct or sinuous, and of the law of resistance in parallel channels. *Phil. Trans. R. Soc. Lond.* **174**, 935–982.

Robinson, S. K. 1991 Coherent motions in the turbulent boundary layer. *Ann. Rev. Fluid Mech.* **23**, 601–639.

Schmiegel, A. 1999 Transition to turbulence in linearly stable shear flows. PhD thesis, Philipps-Universität Marburg.

Tanaka, M. & Kida, S. 1993 Characterization of vortex tubes and sheets. *Phys. Fluids* A **5**, 2079–2082.

Waleffe, F. 1997 On a self-sustaining process in shear flows. *Phys. Fluids* **9**, 883–900.